Printed ISSN 1330–0008
Online ISSN 1333–9125
CD ISSN 1333–8390
CODEN FIZAE4

SCHOTTKY DIODES FABRICATED ON ELECTROCHEMICALLY-GROWN ZnO NANORODS AND MICRORODS

A. E. RAKHSHANI[a], J. KOKAY[a,1] and A. Y. BUMAJDAD[b]

[a]*Physics Department, Faculty of Science, Kuwait University, P.O. Box 5969, Safat 13060, Kuwait*

[b]*Chemistry Department, Faculty of Science, Kuwait University, P.O. Box 5969, Safat 13060, Kuwait*

Received 26 March 2009; Accepted 2 June 2010
Online 12 July 2010

Aligned ZnO nanorods grown on polycrystalline substrates have promising optoelectronic applications. Novel samples with such structures were electrodeposited on stainless foil from a $ZnCl_2$ route. Well-aligned and free-standing hexagonal nanorods with 100 nm diameter and closely-packed microrods with a diameter above 1 μm could be grown normal to the substrate. The optical transition energies (absorption and emission) of samples were determined by transmittance and photoluminescence spectroscopy. We report on the fabrication of high-quality Ag-Schottky diodes formed on the oxygen-treated (002) facets of microrods. Diodes with a large barrier height (1.1 eV), low saturation current density (1.3 pA/cm^2) and high rectification factor (5×10^6 at ± 3 V) were fabricated. The concentration and mobility of free electrons in oxygen-treated microrods were measured as 1.4×10^{14} cm^{-3} and 1.2 cm^{2}V^{-1}s^{-1}, respectively.

PACS numbers: 73.30.+y, 85.30.Kk UDC 537.311

Keywords: hexagonal ZnO nanorods, oxygen-treated (002) facets, high-quality Ag-Schottky diodes, high rectification factor, large barrier height, low saturation current density

1. Introduction

Zinc oxide is a remarkable multifunctional semiconductor with a unique set of properties suitable for applications in a wide range of emerging domains such as solid-state lighting, nanotechnology, transparent electronics and spintronics [1 – 4]. It has a band gap energy of 3.37 eV (300 K) and a large exciton energy of 60 meV.

[1]Corresponding author, E-mail address: kokay@kuc01.kuniv.edu.kw, Phone/fax: 965 5624520

Electrodeposition is a cost-effective method for the growth of calcogenide and oxide films and their nanostructures [5, 9]. To realize ZnO-based devices, the fabrication of high-quality Schottky contacts is essential.

In this work we discuss the structure, optical and electrical properties of aligned ZnO rods vertically grown on stainless steel (SS) foil. The choice of SS foil is due to its low cost and mechanical flexibility and the fact that little is known about the properties of ZnO electrodeposited on SS.

Furthermore, we discuss the characterization of large-barrier Schottky diodes fabricated on the oxygen-treated surface of ZnO rods.

2. Experimental methods

Electrodeposition was performed from 800-ml aqueous $ZnCl_2$ solutions (5 – 9 mM) containing 0.1 M KCl as the supporting electrolyte. The reference and the counter electrodes were Ag/AgCl (SSC) and Pt, respectively. The solution temperature was maintained constant in the range 60 – 80°C for the preparation of different samples. The SS substrate (AISI302), used as a working electrode, was cleaned in an ultrasonic bath of ethanol just before the deposition process which was performed at a cathodic potential of 630 mV to 1000 mV with respect to the reference electrode. The solution was continuously purged with pure oxygen during the deposition period which varied from 50 to 80 minutes. The post-deposition thermal annealing of samples was performed in pure oxygen at atmospheric pressure (400°C, 1 h). Prior to that treatment, samples were immersed in a boiling hydrogen peroxide solution for 3 to 10 minutes.

3. Morphology and structure

Figure 1 shows the morphology of several samples prepared under different conditions listed in Table 1. Sample 1 (Fig. 1a) is composed of aligned nanorods vertically grown on SS. The nanorods with an average length $L = 400$ nm have a hexagonal cross section with a diameter varying in the range 80 – 160 nm (average value $D \approx 100$ nm) and an aspect ratio of $L/D \approx 4$. Figures 1b and 1c show the morphology of the the sample 2 which was prepared from the same solution but under different growth conditions. The rods in the sample 2 have a larger diameter and a lower aspect ratio. As the Zn concentration in the solution increases, the nucleation density on the substrate surface increases as well. This leads to the clustering of nanorods to form rods with a larger diameter. The length of the rods can be controlled by the deposition time, whereas the diameter is a function of deposition parameters, the type of substrate and the solution concentration. Figure 1d shows the plan view of the sample 3 grown from a solution with higher Zn concentration (9 mM). A close examination of the sample 3 reveals that it is formed from closely-packed hexagonal rods covered with a thin ZnO film. Further

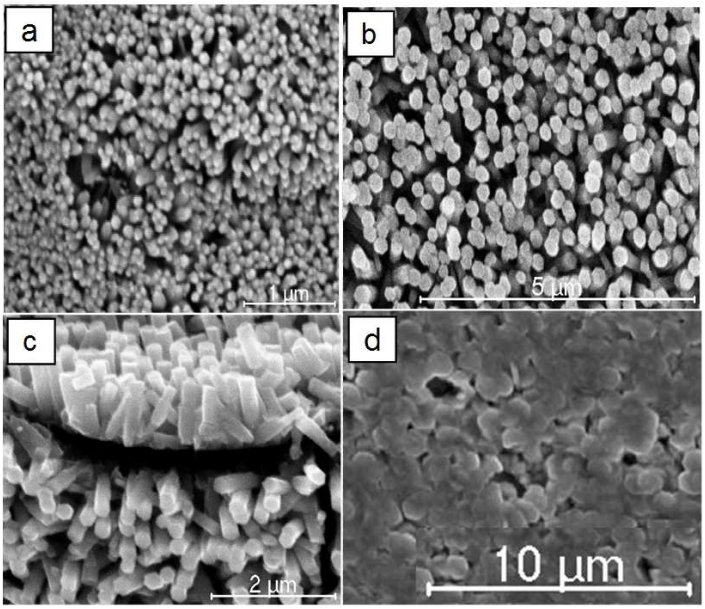

Fig. 1. SEM views from sample 1 (a), sample 2 (b and c) and sample 3 (d) grown under different conditions, as summarized in Table 1.

TABLE 1. Sample deposition parameters: Zinc concentration ([Zn]), *temperature* (T), *deposition potential* (V) *and the average diameter* (D) *and length* (L) *of the grown rods.*

Sample	[Zn] (mM)	T (°C)	$-V$ (mV)	t (min)	D (nm)	L (nm)
1	5	67	730	52	100	400
2	5	83	850	78	200	650
3	9	80	1000	60	1200	1300

deposition would yield a continuous film which can be used as a contact to one end of the arrayed rods, suitable for device applications.

The XRD results obtained on these samples revealed only the (100), (002) and (101) peaks of ZnO wurtzite structure. The EDX technique was used to measure the atomic ratio O/(O + Zn) for different samples. This ratio was obtained as 0.73±0.14 (above the stoichiometric value of 0.5) for the samples 1 and 2 and 0.57 ± 0.09 for the sample 3 which is more stoichiometric than the other two samples. The excess oxygen detected in the samples 1 and 2 could be due to the adsorbed oxygen and OH radicals at the larger surface area of free-standing rods as compared to the compact rods in the sample 3.

4. Optical properties

The spectrum of optical transmittance, T, for the sample 1 is shown in Fig. 2. The nanorods show a good transparency along their c-axis in the visible region. The transmittance shows a sharp absorption onset corresponding to a cut-off wavelength $\lambda_c = 373$ nm which can be used to estimate the rods optical band gap as 3.32 eV. Taken $\ln(T)$ to be proportional to the optical absorption coefficient, the horizontal intercept of the straight-line portion of the left graph shown in the inset of Fig. 2 gives the band gap value of the sample 1 as 3.34 eV. This is very close to 3.37 eV of the bulk ZnO. The second plot in the inset figure measures the band gap of the sample 3 as 3.45 eV. The variation of ZnO band gap with deposition parameters is reported to be in the range 3.27 – 3.55 eV.

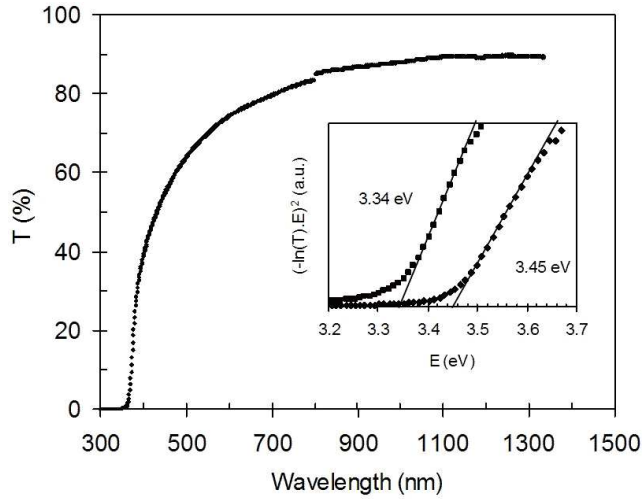

Fig. 2. The optical transmittance spectrum for sample 1. The inset figure shows two plots corresponding to sample 1 (left) and sample 3 (right). T is the optical transmittance and E the photon energy.

The room-temperature photoluminescence spectrum of the sample 1 is shown in Fig. 3. The spectrum of the as-grown sample (inset) shows a peak at 378 nm (3.28 eV) with FWHM = 30 nm and a broad peak at about 580 nm. The UV peak is assigned to the electron transition from a defect level, 0.09 eV below the conduction band (taking the band gap 3.37 eV), to the valence band. This defect level is likely the prominent donor-type level E1 in ZnO which is located 0.12 eV below the conduction band edge, in agreement with our previous results 0.11 – 0.12 eV [10 – 12]. The broad peak in Fig. 3 is the defect-related visible emission characteristic of ZnO. This defect level, which can also be observed in chemically-grown ZnO films, is most likely associated with the doubly-ionized oxygen-vacancy defects (V_O^{2+}) located 2.2 eV below the conduction band edge [11, 13]. Thermal annealing in air or in pure oxygen (400°C, 1 h) suppresses this emission and enhances the intensity of the UV peak.

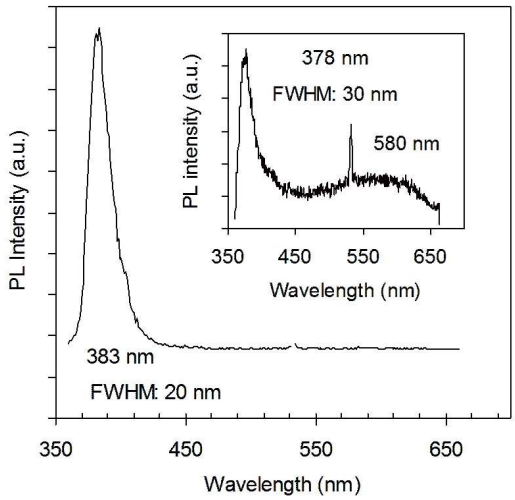

Fig. 3. The room-temperature photoluminescence of sample 1, before (inset) and after anneaing in air for 1 h *at* 400°C. *The sharp peak at* 532 nm *is the second harmonic of the excitation source.*

5. *Schottky-diode characteristics*

Figure 4 shows schematically the structure of Schottky contacts prepared on the samples 1 and 3. Silver contacts were deposited after a brief surface treatment of the samples in boiling hydrogen peroxide.

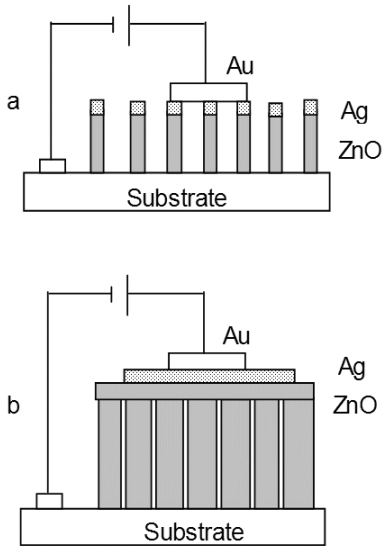

Fig. 4. The schematic diagrams showing the structure of silver Schottky contacts prepared on a) sample 1 and b) sample 3. The top contact shown represents a spring-loaded gold probe.

The current-voltage (I-V) characteristics of a device prepared on the sample 3 are shown in Fig. 5. The device shows a good rectification factor $R = 5.35 \times 10^6$ at $\pm$ 3V. The (I-V) characteristic of an ideal Schottky diode is given by

$$I = I_0 \left\{ \exp\left[q \frac{V - IR_s}{nkT} \right] - 1 \right\}, \tag{1}$$

where q is the electronic charge, n the ideality factor, k the Boltzmann's constant, T the absolute temperature and R_s the diode series resistance. The saturation current, I_0, when governed by thermionic emission, is given by

$$I_0 = AA^*T^2 \exp\left(-\frac{q\Phi}{kT} \right), \tag{2}$$

where A is the device active area, A^* the effective Richardson constant ($A^* = 32$ Acm^{-2}K^{-2} for ZnO) and Φ is the zero-field barrier height. The barrier height and the ideality factor of the diode in Fig. 5 were obtained as $\Phi = 1.09$ V and $n = 2.2$ by fitting to (1) and (2) the forward I-V data in the current range 10 nA – 10 μA, where the effect of series resistance is negligible. The saturation current density of the device $J_0 = I_0/A = 1.3$ pAcm^{-2} is remarkably low. From (1) it can be shown that

$$\frac{I}{\mathrm{d}I/\mathrm{d}V} = R_s I + \frac{nkT}{q}.$$

A plot of $\dfrac{I}{\mathrm{d}I/\mathrm{d}V}$ against I yielded a straight line from which $R_s = 490$ Ω was obtained.

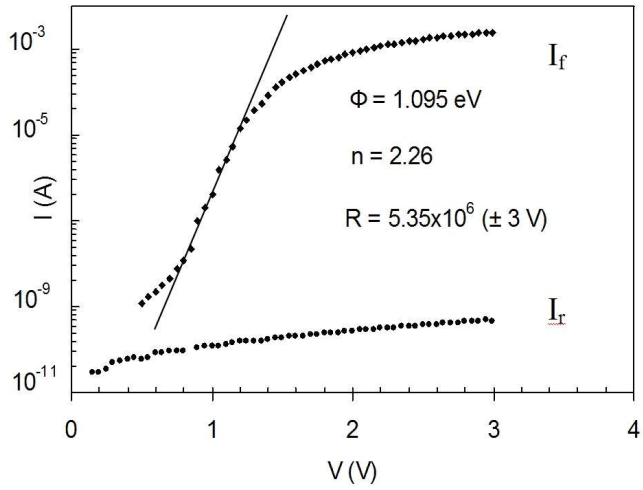

Fig. 5. The current-voltage characteristics in the forward (I_f) and reverse directions (I_r) for a Schottky diode fabricated on sample 3.

Figure 6 shows the capacitance-voltage characteristics of the device in Fig. 5 measured at two different frequencies. The junction built-in potential, V_0, and the concentration of uncompensated donors, N_d, in the sample 3 were measured as $V_0 = 0.93$ V and $N_d = 1.4 \times 10^{14}$ cm^{-3} from the fit of the 100 kHz C-V plot to the theoretical relationship given as

$$C^{-2} = \frac{2}{q\epsilon_r\epsilon_0 N_d A^2} \left(V_0 - \frac{kT}{q} - V \right). \tag{3}$$

Here, ϵ_0 is the permittivity of free space and ϵ_r is the low-frequency dielectric constant of ZnO taken as 8.0 at 100 kHz. Using the same N_d value, the slope of the 1-MHz C-V plot measures the high-frequency dielectric constant as $\epsilon_r = 4.0$, in good agreement with the literature value of 3.7. Taking $N_d = 1.4 \times 10^{14}$ cm^{-3}, $N_c = 2.94 \times 10^{18}$ cm^{-3} (effective density of states in the conduction band of ZnO) and using $\zeta = (kT/q)\ln(N_c/N_d)$, the position of the Fermi level from the conduction band was determined as $\zeta = 0.23$ eV. From the device physical dimensions and the measured values of $R_s = 490\ \Omega$ and $N_d = 1.4 \times 10^{14}$ cm^{-3} and taking the free-electron concentration $n = N_d$, the resistivity and the electron mobility values are estimated at $3.7 \times 10^4\ \Omega$cm and $\mu = 1.2$ cm^{2}V^{-1}s^{-1}, respectively.

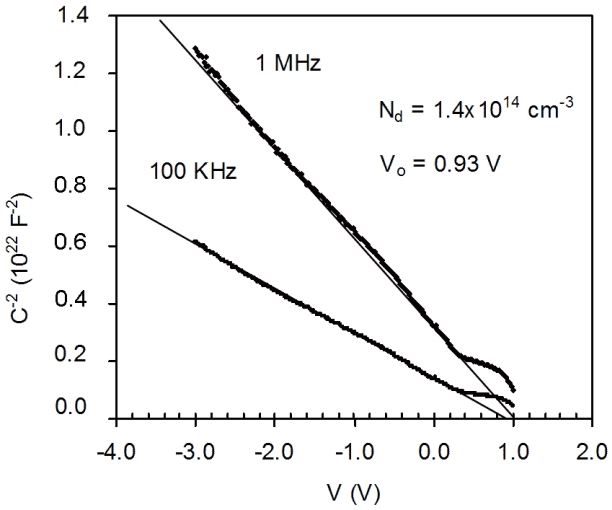

Fig. 6. The capacitance-voltage (C-V) characteristics of the device in Fig. 5, measured at 100 kHz *and* 1 MHz.

Silver Schottky diodes with a configuration shown in Fig. 4a were prepared on the sample 1. The I-V and C-V characteristics of a device shown in Fig. 7 reveal the formation of Schottky contacts on the (002) facets of nanorods.

The relatively low rectification factor (30 at ± 1.5 V) in the I-V plot is likely due to the low shunt resistance of the device, which in turn is due to the partial deposition of Ag on the stems of nanorods. The analysis of the forward I-V char-

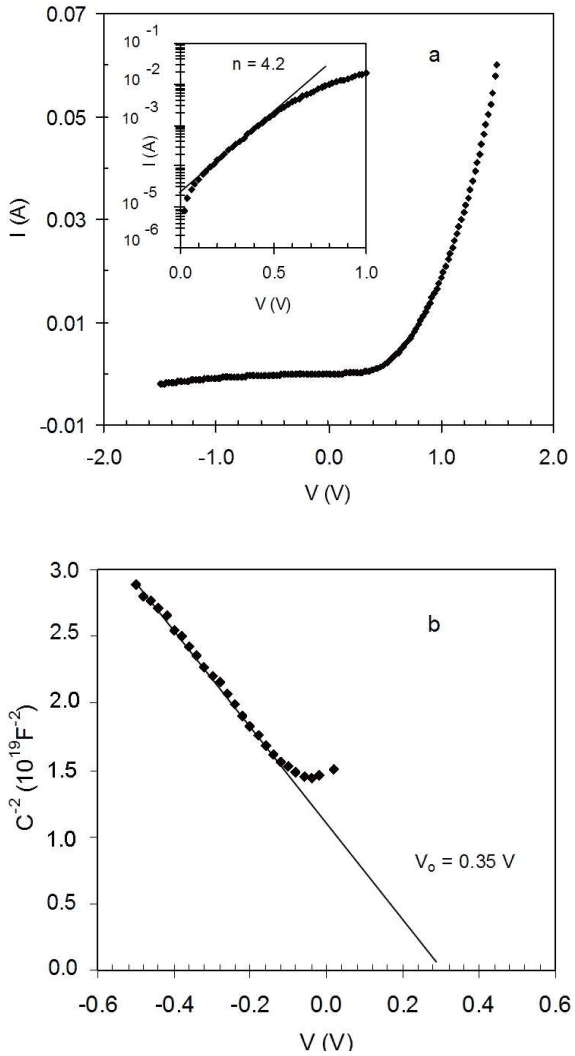

Fig. 7. The current-voltage (a) and the capacitance-voltage (100 kHz) characteristics (b) of a Schottky diode prepared on nanorods (sample 1).

acteristic gives an ideality factor $n = 4-5$ and a relatively large saturation current $I_0 = 22$ A. The C-V plot yields a relatively small built-in potential $V_0 = 0.35$ V. Due to uncertainty on the device active area, A, which depends on the number of Ag-capped ZnO nanorods in electrical contact with the Au-plated probe, the values of Ω and N_d can not be obtained from Eqs. (2) and (3). To achieve better diodes on nanorod samples, the work is in progress to fill up the empty space between the nanorods with an insulating polymer before the deposition of Ag contact.

6. Conclusion

Hexagonal nanorods deposited on the substrate by electrodeposition are studied. Characterization using optical and spectroscopic methods has shown that they are packed closely and aligned perpendicularly to the surface of the substrate. Here we report a high quality Schottky diode made by mentioned micro and nanorods. The barrier height of the obtained diode seems to have a large height and low saturation cornet density.

The florescence spectroscopy has shown that the obtained structure has a band gap energy of 3.7 eV and a large exciton energy. The current-voltage and capacitance-voltage characteristics obtained for our diode suggest its possible application in the future. They have a promising application for making optoelectronic devices and detectors.

Acknowledgements

We thankfully acknowledge the Kuwait University funded research project SP01/06 and the general-facility projects GS01/01 and GS03/01. We also acknowledge the use of facilities in the Electron Microscopy Unit.

References

[1] Ü. Özgür, Y. I. Alivov, C. Liu, A. Teke, M. A. Reshchikov, S. Doğan, V. Avrutin, S.-J. Cho and H. Morkoçd, J. Appl. Phys. **98** (2005) 041301.

[2] Z. L. Wang, J. Phys. D: Condens. Matter **16** (2004) R829.

[3] L. Schmidt-Mende and J. L. MacManus-Driscoll, Mater. Today **10** (2007) 40.

[4] M. C. Newton and P. A. Warburton, Mater. Today **10** (2007) 50.

[5] D. Lincot, Thin Solid Films **487** (2005) 40.

[6] T. Pauporte and D. Lincot, Electrochim. Acta **45** (2000) 3345.

[7] M. W. Allen et al., IEEE Trans. Electron Devices, **56**, 9 (2009) 2160.

[8] E. V. Monakhov, A Yu Kuznetov and B. G Svensson, J. Physics D: Applied Physics **42** (2009) 15300.

[9] D. M. Hofmann, A. Hofstaetter, F. Leiter, H. Zhou, F. Henecker, B. K. Meyer, S. B. Orlinskii, J. Schmidt and P. G. Baranov, Phys. Rev. Lett. **88** (2002) 504

[10] A. E. Rakhshani, Appl. Phys. A **81** (2005) 1497.

[11] A. E. Rakhshani, J. Kokaj, J. Mathew and B. Peradeep: Appl. Phys. A **86** (2007) 377.

[12] J. Kokaj and A E Rakhshani, J. Phys. D: Apl. Phys. **23** (2004) 378.

[13] A. E. Rakhshani, A. Bumajdad and J. Kokaj, Appl. Phys. A **89** (2007) 923.

SCHOTTKYJEVE DIODE PROIZVEDENE NA ELEKTRO-KEMIJSKI RASLIM NANO- I MIKRO-ŠTAPIĆIMA

Poredani nanoštapići ZnO, narasli na polikristalnoj podlozi, mogli bi naći primjene u optoelektroničkim napravama. Pripremili smo nove uzorke takvih naprava elektro-taloženjem na listiće nerđajućeg čelika primjenom $ZnCl_2$. Postigli smo dobro odvojene i poredane heksagonalne nano-štapiće promjera 100 nm i gusto poredane mikro-štapiće promjera većeg od 1 μm, narasle okomito na podlogu. Primjenom propusne i fotoluminescentne spektroskopije odredili smo (apsorpcijske i emisijske) prijelazne energije uzoraka. Izvješćujemo o izradi visoko-kvalitetnih Ag-Schottky dioda izvedenih na (002) plohama mikro-štapića nakon obrade kisikom. Načinili smo diode s visokim protunaponom (1.1 eV), malom gustoćom struje zasićenja (1.3 pA/cm^2) i velikim faktorom ispravljanja (5×10^6 na ± 3 V). Odredili smo koncentraciju i pokretljivost slobodnih elektrona u kisikom-obrađenim mikro-štapićima od 1.4×10^{14} cm^{-3} odnosno 1.2 cm^{2}V^{-1}s^{-1}.